J Mater Sci: Mater Electron (2015) 26:3025–3034
DOI 10.1007/s10854-015-2793-x

Effects of Bi^{3+} doping of the dielectric and piezoelectric properties of $Ba_{0.9}Ca_{0.1}Ti_{0.9}Zr_{0.1}O_3$ ceramics prepared by hydrothermal method

Yuwen Liu · Yongping Pu · Zixiong Sun · Qian Jin

Received: 13 November 2014 / Accepted: 31 January 2015 / Published online: 7 February 2015

Abstract Ceramics in the solid solution system, $Ba_{0.9}Ca_{0.1}Ti_{0.9}Zr_{0.1}O_3$–$xBi^{3+}$ ($x = 0.000$–0.030) were prepared by hydrothermal and were assisted by microwave sintering. Effects of Bi^{3+} content on the phase transition, microstructure, and electrical properties of ceramics were investigated. The single phase perovskite-type ceramics showed different polymorphs and the grain size was significantly influenced with the doping of Bi^{3+}. Dielectric measurements indicated excellent dielectric relaxation behavior for $x = 0.005$ and $x = 0.030$. At $x = 0.015$ and $x = 0.020$, samples show giant dielectric constant (near 200,000) and lower dielectric loss (lower than 1.2), compared with other giant permittivity materials such as CCTO. The relationship between T_C and $2E_C$ was investigated and a novel conclusion of the $2E_C$ was increased with increasing T_C was reached. A maximum value of $d_{33} = 265$ pC/N was observed at $x = 0.025$ for the emergence of T_{O-T}. That is because piezoelectrics always possessed high d_{33} near morphotropic phase boundary.

1 Introduction

Due to their attractive physical properties, such as high dielectric permittivity, diffuse phase transition and strong electrostriction, relaxor ferroelectric materials have attracted special attention during the last few decades. Most of these materials belong to complex lead-based perovskite compounds, such as PMN-PT and PMN-PZT, whose superior dielectric properties and relaxor behaviour have had considerable contributions in the development of relaxor ferroelectric materials [1–4]. For a half century, Pb-based piezoelectric ceramics, such as lead zirconium titanate [$PbTiO_3$–$PbZrO_3$ (PZT)], have dominated the field of piezoelectric ceramics worldwide. Because of its high d_{33} and k_p, PZT have been successfully applied in a wide range of systems and technologies, including sensors, actuators, transducers, and memory elements. These materials have, however, often been reported to pose a number of environmental and health concerns due to the volatility and toxicity of lead [5–7].

These disadvantages have motivated the search for new, efficient, and eco-friendly lead-free relaxor ferroelectric materials and piezoelectric materials. Several lead-free materials with perovskite structure, such as $Ba_{1-x}Sr_xTiO_3$–Bi have been investigated, and in 2009, BCTZ ferroelectric system with a super high d_{33} was designed, and since then, BCTZ system materials have attracted considerable attention and been considered as one of the promising candidates for lead-free piezoelectric ceramics. However, relaxor ferroelectric materials always show poor piezoelectric properties and there is little work to combine these two properties in one single materials [7–13].

In present work, the $Ba_{0.9}Ca_{0.1}Ti_{0.9}Zr_{0.1}O_3$–$xBi^{3+}$ ceramics were prepared by hydrothermal method and were assisted by fast microwave sintering method. Compared with the conventional method, the hydrothermal method has advantages of high purity and homogeneous grain size in synthesizing powders. Microwave sintering (MS) is a unique technique alternative to the conventional sintering, by which the heat is generated internally within the material through microwave–material interaction instead of originating from external sources [14, 15]. It is particularly a suitable sintering method for the ceramics with ultrafine

Y. Liu (✉) · Y. Pu · Z. Sun · Q. Jin
School of Materials Science and Engineering, Shaanxi University of Science and Technology, Xi'an 710021, People's Republic of China
e-mail: 15502966389@163.com

powders prepared by hydrothermal method. The $Ba_{0.9}Ca_{0.1}Ti_{0.9}Zr_{0.1}O_3$–$xBi^{3+}$ ceramics in this study show excellent relaxor behavior as well as high d_{33} with $x = 0.005$ and $x = 0.030$.

2 Experimental

$Ba_{0.9}Ca_{0.1}Ti_{0.9}Zr_{0.1}O_3$–$xBi^{3+}$ ceramics were prepared by hydrothermal method and the $BaCl_2{\cdot}2H_2O$ (SCRC), $CaCl_2$, $TiCl_4$, $ZrOCl_2{\cdot}8H_2O$ and $Bi(NO_3)_3$ were used as raw materials. $BaCl_2{\cdot}2H_2O$, $CaCl_2$ $ZrOCl_2{\cdot}8H_2O$ and $Bi(NO_3)_3$ were first dissolved in distilled water respectively and then were mixed. The $TiCl_4$ was added into the mixtures dropwise to obtain $Ba_{0.9}Ca_{0.1}Ti_{0.9}Zr_{0.1}O_3$–$xBi^{3+}$ precursors. Finally the NaOH was added to regulated the pH > 14. The three precursors were put into the heating-autoclave, followed by distilled water until the total volume reached to ~80 % of the autoclave. The hydrothermal reactions were carried out at 180 °C for 10 h and finally the three powders were mixed before dried. After that, the powders were pressed into pellets of 12 mm diameter and the pellets were sintered at 1280 °C for 10 min under microwaves.

Phase structure of $Ba_{0.9}Ca_{0.1}Ti_{0.9}Zr_{0.1}O_3$–$x$La ceramics was examined using an X-ray diffraction (D/max 2200 pc, Rigaku, Tokyo, Japan) with CuKα radiation. The microstructure morphologies were obtained by scanning electron microscopy (JEOL JSM-6390A JEOL Ltd. Tokyo), and the densities were measured according to Archimedes principle. Dielectric and ferroelectric measurements were carried by Agilent 4980A impedance analyzer and a ferroelectric analyzer (Premier II, Radiant, USA). The ceramics were poled under a DC field of 4 kV/mm in silicon oil bath for 10 min at different temperatures and the d_{33} of the poled ceramics was measured using a quasi-static meter d_{33} meter (ZJ-4AN, China).

3 Results and discussion

The XRD patterns of the $Ba_{0.9}Ca_{0.1}Ti_{0.9}Zr_{0.1}O_3$–$xBi^{3+}$ ceramics are shown in Fig. 1. All the ceramics have pure perovskite structure and no second phases were detected, suggesting that Bi^{3+} was incorporated into the BCTZ lattices to form a solid solution. The $Ba_{0.9}Ca_{0.1}Ti_{0.9}Zr_{0.1}O_3$–$xBi^{3+}$ ceramics exhibit different polymorphs with different x: Samples with $x = 0.000$ and $x = 0.020$ show single orthorhombic (O) phase for the narrow and single (002)/(200) peak. The broadening peak with (002)–(200) less than 1 indicates the coexistence of tetragonal (T) and cubic (C) phase for $x = 0.005$, $x = 0.010$ and $x = 0.030$. Samples with $x = 0.015$ and $x = 0.025$ possess single tetragonal phase and the coexistence of orthorhombic and tetragonal phase respectively, which is characterized by the (002)–(200) is greater than 1 and is approximate to 1 [2–4]. And these will be studied detailedly in temperature dependence of dielectric constant in the following discussion. The radius of Bi^{3+} (0.117 nm) is very close to those of Ba^{2+} (0.161 nm) and Ca^{2+} (0.134 nm) in A site of the BCTZ ceramics and therefore Bi^{3+} most likely occupy the A sites firstly with smaller amount of addition according to the principles of crystal chemistry [4–9]. With further addition of Bi^{3+}, it maybe probably enter the oxygen octahedron for substituting Ti^{4+} and Zr^{4+} for the saturated solid solubility in A site. It is also noticed that the (200)/(002) peak shifts towards higher degree of 2θ with increasing Bi^{3+} content for the decreasing lattice parameter d.

Figure 2 shows SEM micrographs (a–g) of thermally etched surface for $Ba_{0.9}Ca_{0.1}Ti_{0.9}Zr_{0.1}O_3$–$xBi^{3+}$ ceramics ($0.000 \le x \le 0.030$) and the corresponding average grain size (h), and the grain size was measured using the Mean Lineal Intercept Method (ASTM Standard E112-88). It can be observed that the grain size is influenced significantly with the introduction of Bi^{3+}. The sample with $x = 0.005$ possesses smaller and more homogeneous grain size compared with Bi^{3+} free sample and the grain size is increased sharply to ~7.8 μm when $x = 0.010$. With further doping, the grain size decreases gradually again. These phenomenons can be understood as follows: The grain size of $Ba_{0.9}Ca_{0.1}Ti_{0.9}Zr_{0.1}O_3$ ceramics firstly decreased for the refining mechanism of micro-doping of Bi^{3+}, and then increased significantly at $x = 0.010$ because of the reduction of interfacial free energy [2, 4]. With further increasing x, more Bi^{3+} dissolved in $Ba_{0.9}Ca_{0.1}Ti_{0.9}Zr_{0.1}O_3$ lattice at high temperature during sintering process, while in the cooling step, extra Bi^{3+} separated out and aggregated in grain boundaries, the migration of grain boundaries was inhibited and thus the grain growth was decreased.

Figure 3 shows the dielectric constant of $Ba_{0.9}Ca_{0.1}Ti_{0.9}Zr_{0.1}O_3$–$xBi^{3+}$ ceramics as a function of temperature measured at frequencies 1, 10, 100 and 1,000 kHz respectively (a–g), and T_C and resistivity as a function of x (h). Some novel phenomenons can be observed: Plots of Fig. 3a, e indicate $Ba_{0.9}Ca_{0.1}Ti_{0.9}Zr_{0.1}O_3$–$xBi^{3+}$ ceramic with $x = 0.000$ $x = 0.025$ of single transition peak with wide T_C range, which is agreed with former literatures [3–9]. While sample of $x = 0.025$ exhibits two phase peaks of T_C and T_{O-T} (orthorhombic to tetragonal), suggesting the coexistence of orthorhombic and tetragonal phase at room temperature, which is agreed with the conclusions of XRD. Samples of $x = 0.010$ and $x = 0.015$ can be used as giant permittivity materials, and judging from the significant disparity of permittivities between different frequencies, it can be assumed that the giant dielectric behavior results

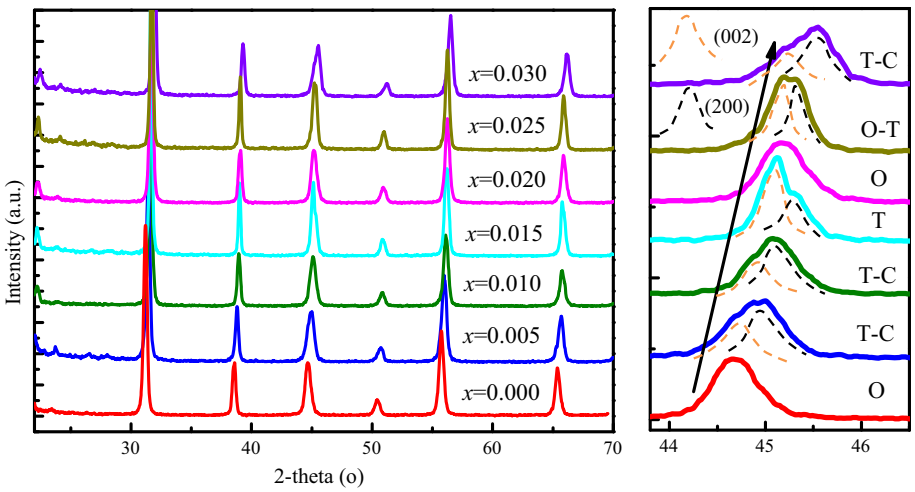

Fig. 1 X-ray patterns of the $Ba_{0.9}Ca_{0.1}Ti_{0.9}Zr_{0.1}O_3$–$xBi^{3+}$ ceramics with different x

from some relaxation polarizations with the addition of Bi^{3+}. As our earlier research [10, 11], the defect chemical reactions of Bi^{3+} (donor doping) for A-site ions at higher x are represented as:

$$Bi^{3+} \xrightarrow{Ba^{2+}} Bi^{\cdot\cdot}_{Ba} + e' \quad Bi^{3+} \xrightarrow{Ca^{2+}} Bi^{\cdot\cdot}_{Ca} + e'$$

$$4Bi^{3+} \xrightarrow{Ba^{2+}} 4Bi^{\cdot\cdot}_{Ba} + V^{''''}_{Ti} \quad 4Bi^{3+} \xrightarrow{Ca^{2+}} 4Bi^{\cdot\cdot}_{Ca} + V^{''''}_{Zr}$$

Relaxation polarizations such as dipole polarization and space charge polarization caused by the emergence of e' and $V^{''''}_{Ti}$ cannot keep pace up with the electrical field with higher frequency, only making contribution in increasing the permittivity significantly of samples at $f = 1$ kHz and $f = 10$ kHz. Figure 3h indicates that the resistivity of $Ba_{0.9}Ca_{0.1}Ti_{0.9}Zr_{0.1}O_3$–$xBi^{3+}$ ceramics decreases firstly and then increases with increasing Bi^{3+} content, exhibiting the minimum value at $x = 0.010$ of 2.7×10^2 Ω cm. The sharp decreasing of resistivity is due to the e' and $V^{''''}_{Zr}$ serving as carriers in ceramics, and the sample with the lowest resistivity always exhibits the largest grain size in BCTZ ceramics with donor doping. With the further doping of Bi^{3+} in the A site of BCTZ ceramics, the carriers disappeared and the so did the PTC behavior. The samples became to dielectrics again. Both the permittivities and the T_c decreased and the P–E loops can also be detected. This variation is in accordance with the former literature [12, 13]. Plots of Fig. 3b, g indicate that $Ba_{0.9}Ca_{0.1}Ti_{0.9}Zr_{0.1}O_3$–$xBi^{3+}$ solid solutions with $x = 0.005$ and $x = 0.030$ are relaxor ferroelectrics with excellent frequency dispersion and diffused phase transition.

The relaxation behaviors at 10 kHz of $Ba_{0.9}Ca_{0.1}Ti_{0.9}Zr_{0.1}O_3$–$xBi^{3+}$ ceramics with $x = 0.005$ and $x = 0.030$ are shown in Fig. 4. Plots of inverse dielectric permittivity versus temperature are shown in (a) and (b). The deviation from the Curie–Weiss law for relaxor ferroelectrics can be defined by ΔT_m as follows:

$$\Delta T_m = T_{cm} - T_m, \tag{1}$$

where T_{cm} refers to the temperature from which dielectric permittivity starts to deviate from the Curie–Weiss law and T_m to the temperature at which dielectric permittivity reaches the maximum [4]. The ΔT_m value calculated at 10 kHz was 37 and 30 °C for $x = 0.005$ and $x = 0.030$ respectively, and was noted to be almost invariable with the increase in frequency. The dielectric characteristics of relaxor ferroelectrics are known to deviate from the typical Curie–Weiss behavior and can be well described by the Uchino and Nomura function, a modified Curie–Weiss relationship:

$$1/\varepsilon - 1/\varepsilon_m = (T - T_m)\gamma/C \quad 1 < \gamma < 2 \tag{2}$$

where ε_m refers to the maximum value of dielectric permittivity, ε to the dielectric permittivity at temperature T, T_m to the temperature at the peak of the dielectric permittivity, C to the Curie constant, and γ to the diffuseness degree indicator, taking the value between 1 (for a normal ferroelectric) and 2 (for a complete diffuse phase transition). The value of γ can, therefore, be used to characterize the relaxor behavior [2, 5]. The plot of ln $(1/\varepsilon - 1/\varepsilon_m)$ as a function of ln $(T - T_m)$ is shown in (c) and (d). By fitting the Uchino equation, the exponent γ which determines the diffuseness degree of the phase transition, was obtained from the slope of log ln$(1/\varepsilon - 1/\varepsilon_m)$-vs-ln$(T - T_m)$ plots. The value obtained for the parameter was 1.65 and 1.74, suggesting that samples with $x = 0.005$ and $x = 0.030$ are relaxor ferroelectric with strong diffuse phase transition. The ΔT_{relax} was also introduced to investigate the relaxor feature of the two samples, and The degrees of relaxation behaviour and diffuseness were defined as:

$$\Delta T_{relax} = T/\varepsilon_m(1000\ \text{kHz}) - T/\varepsilon_m(1\ \text{Hz}) \tag{3}$$

Based on the experimental data, the values calculated for ΔT_{relax} are 13 °C and 15 °C for $x = 0.005$ and

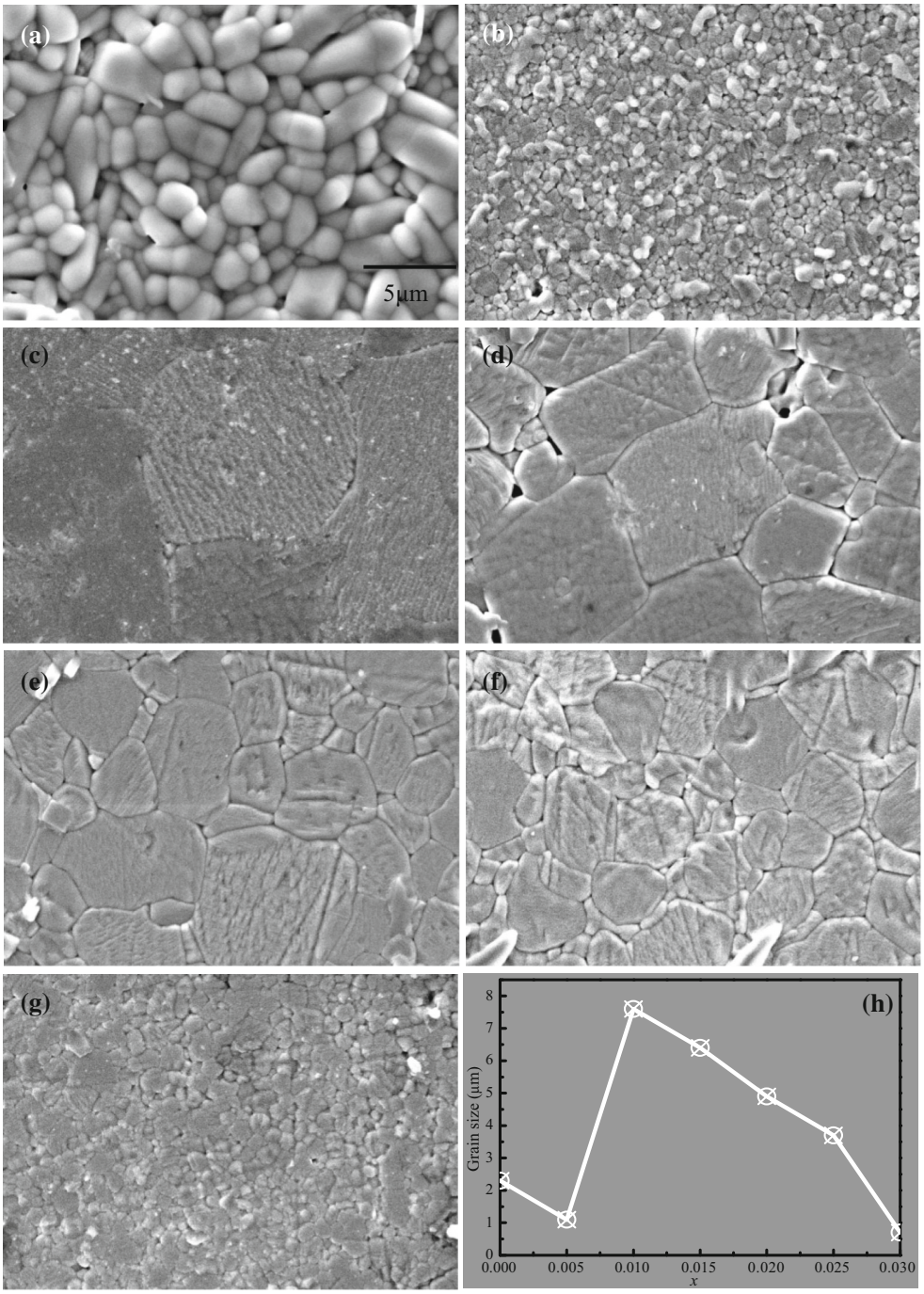

Fig. 2 **a–g** SEM micrographs of the $Ba_{0.9}Ca_{0.1}Ti_{0.9}Zr_{0.1}O_3$–$xBi^{3+}$ ceramics with different x: (a) $x = 0.000$; (b) $x = 0.005$; (c) $x = 0.010$; (d) $x = 0.015$; (e) $x = 0.020$; (f) $x = 0.025$; (g) $x = 0.030$. **h** Relationship between x and average grain size

$x = 0.030$ respectively. The temperature of maximum permittivity versus ln$f$ for $x = 0.005$ and $x = 0.030$ are shown in Fig. 4e. These excellent dielectric relaxor behaviors are attributed to the structural fluctuation caused by more homogeneous grain size, which is shown in Fig. 2b, g.

On the basis of the relationship between ln$f$ and T_C, we can calculate the relaxor activated parameters of the T_C peak. For a relaxation process, the relaxation time generally follows the Arrhenius law:

$$\tau = \tau_0 \exp(E/K_B T) \quad (4)$$

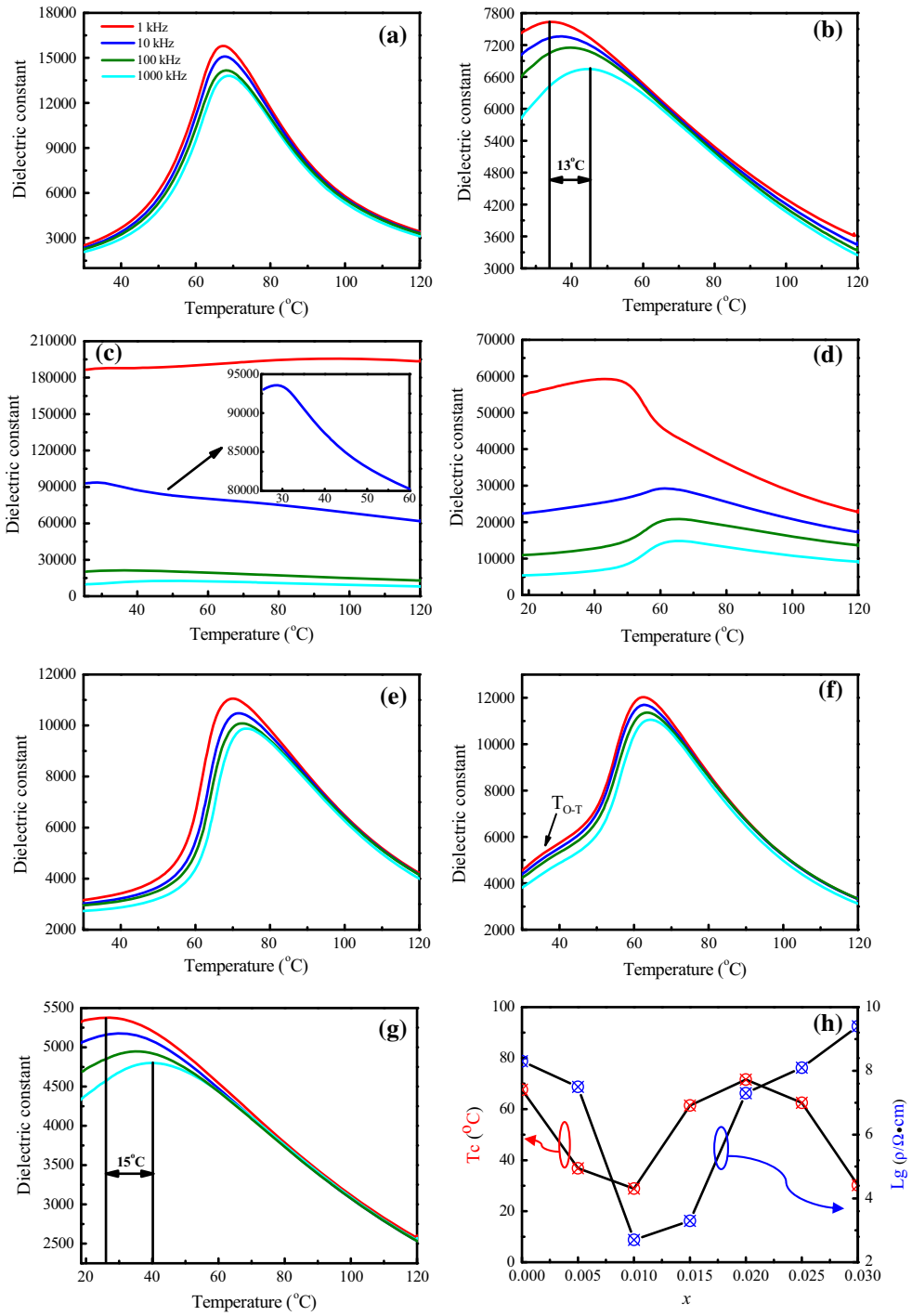

Fig. 3 **a–g** Temperature dependence of dielectric constant for the $Ba_{0.9}Ca_{0.1}Ti_{0.9}Zr_{0.1}O_3$–$xBi^{3+}$ ceramics with different x: (a) $x = 0.000$; (b) $x = 0.005$; (c) $x = 0.010$; (d) $x = 0.015$; (e) $x = 0.020$; (f) $x = 0.025$; (g) $x = 0.030$. **h** T_C and resistivity as a function of x

where τ_0 is the pre-exponential factor (or the relaxation time at infinite temperature), E denotes the activation energy of the relaxation process, T is the absolute temperature, and K_B is the Boltzmann constant. The condition $\omega_p\tau_p = 1$ is fulfilled at the peak position, where $\omega = 2\pi f$ is the angular frequency of measurement and the subscript p denotes values at peak position. If we plot the $\ln(\omega_p)$ as a function of the reciprocal of peak temperature (Arrhenius plots), a linear relation would be obtained. The relaxation parameters E and τ_0 can thus be deduced from the slope and intercept of this line, respectively [4, 5, 15, 17, 19]. Figure 4f, g shows the Arrhenius plots for the dielectric constant peak, where the solid line is the result of a linear least-square fitting. The relaxation parameters $E = 4.24$ eV; $\tau_0 = 3.32 \times 10^{-14}$ s for $x = 0.005$ and $E = 3.68$ eV; $\tau_0 = 3.34 \times 10^{-14}$ s for $x = 0.030$ are obtained from the fitting line.

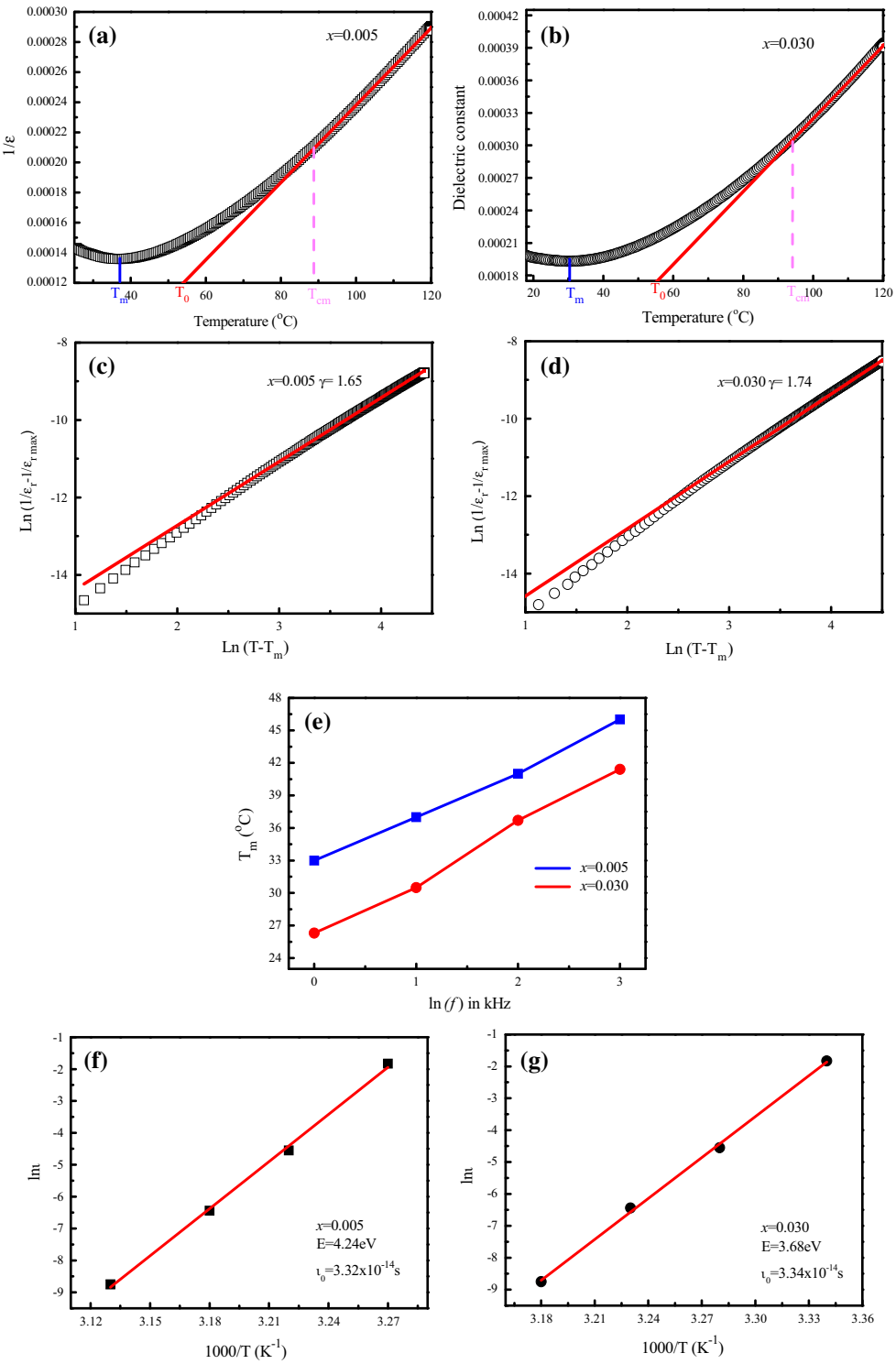

Fig. 4 **a**, **b** The plot of the inverse dielectric constant versus temperature at 10 kHz: (a) $x = 0.005$; (b) $x = 0.030$. **c**, **d** $\ln(1/\varepsilon - 1/\varepsilon_m)$ as a function of $\ln(T - T_m)$ at 10 kHz: (c) $x = 0.005$; (d) $x = 0.030$. **e** Temperature of maximum permittivity, versus ln*f* for $x = 0.005$ and $x = 0.030$. **f**, **g** Arrhenius plot of the dielectric relaxation peak from the frequency spectra: (f) $x = 0.005$; (g) $x = 0.030$

Figure 5 shows the dielectric loss of $Ba_{0.9}Ca_{0.1}Ti_{0.9}Zr_{0.1}O_3$–$xBi^{3+}$ ceramics as a function of temperature measured at frequencies 1, 10, 100 and 1,000 kHz respectively. Figure 5a, e shows single peak (T_C) while (f) shows two peaks (T_C and T_{O-T}), which is agreed with Fig. 3. Contrary to the others, the dielectric loss increases with increasing frequency in (b) and (g), which is a character of relaxor ferroelectrics. Figure 5c indicates the highest dielectric loss of $x = 0.015$, which caused by the relaxation polarizations as discussed above. $Ba_{0.9}Ca_{0.1}Ti_{0.9}Zr_{0.1}O_3$–$0.015Bi^{3+}$ ceramic shows giant dielectric behavior especially in low frequencies and dielectric loss

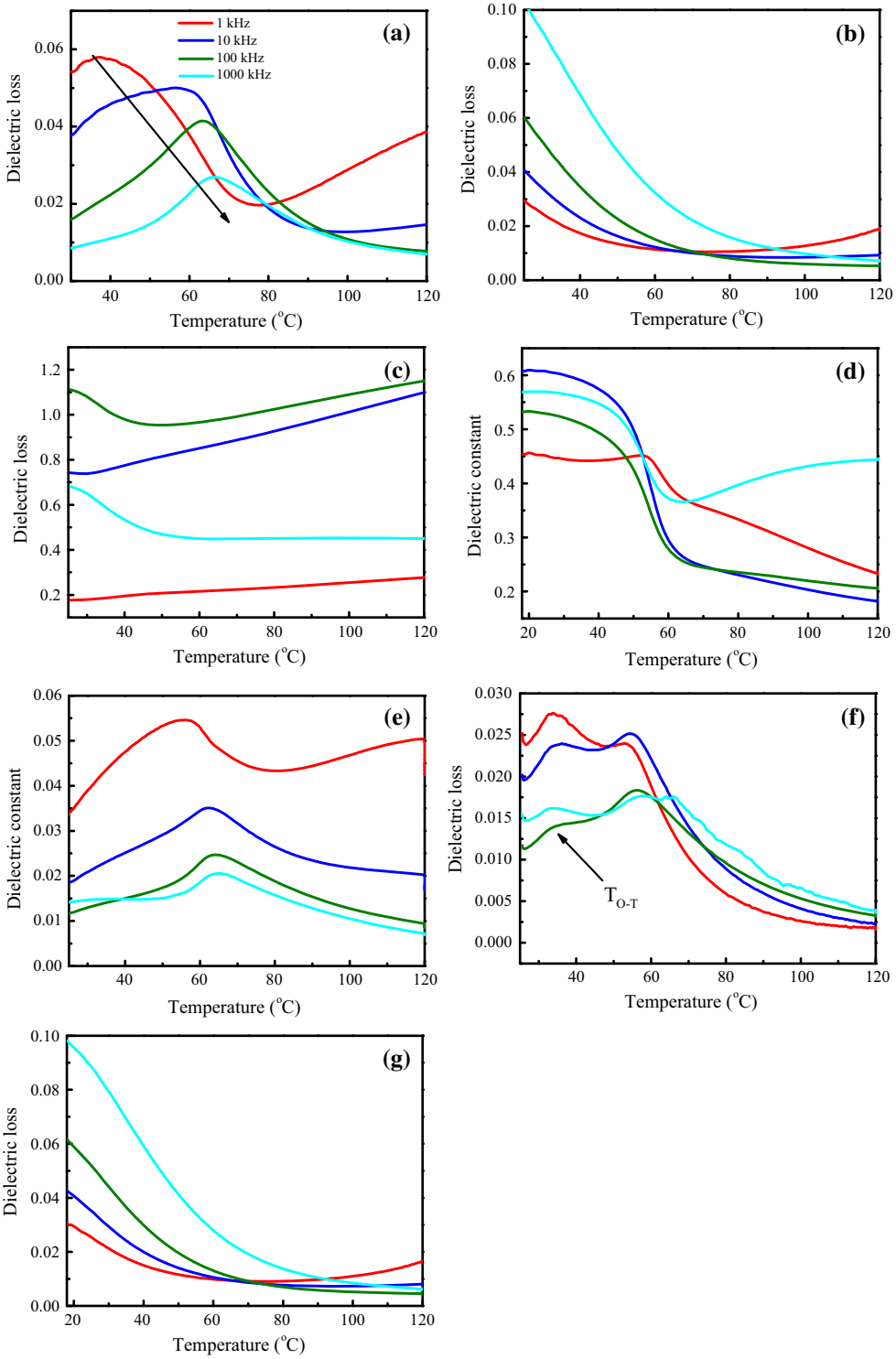

Fig. 5 Temperature dependence of dielectric loss for the $Ba_{0.9}Ca_{0.1}Ti_{0.9}Zr_{0.1}O_3$–$xBi^{3+}$ ceramics with different x: (a) $x = 0.000$; (b) $x = 0.005$; (c) $x = 0.010$; (d) $x = 0.015$; (e) $x = 0.020$; (f) $x = 0.025$; (g) $x = 0.030$

lower than 0.6. Compared with other giant dielectric constant materials such as $CaCu_3Ti_4O_{12}$ (CCTO), which shows dielectric loss over 10, this materials has advantages in much higher dielectric constant and lower dielectric loss.

Figure 6 shows the ferroelectric hysteresis loops measured at room temperature of the $Ba_{0.9}Ca_{0.1}Ti_{0.9}Zr_{0.1}O_3$–$xBi^{3+}$ ceramics with $x = 0.000$, 0.005, 0.020, 0.025 and 0.030, and all these samples possess a typical ferroelectric polarization hysteresis loop. Ferroelectric properties can not be detected in samples with $x = 0.010$ and $x = 0.015$ for the lower resistivity as shown in Fig. 3h. In this case, the ceramics are easily to be broken down under a

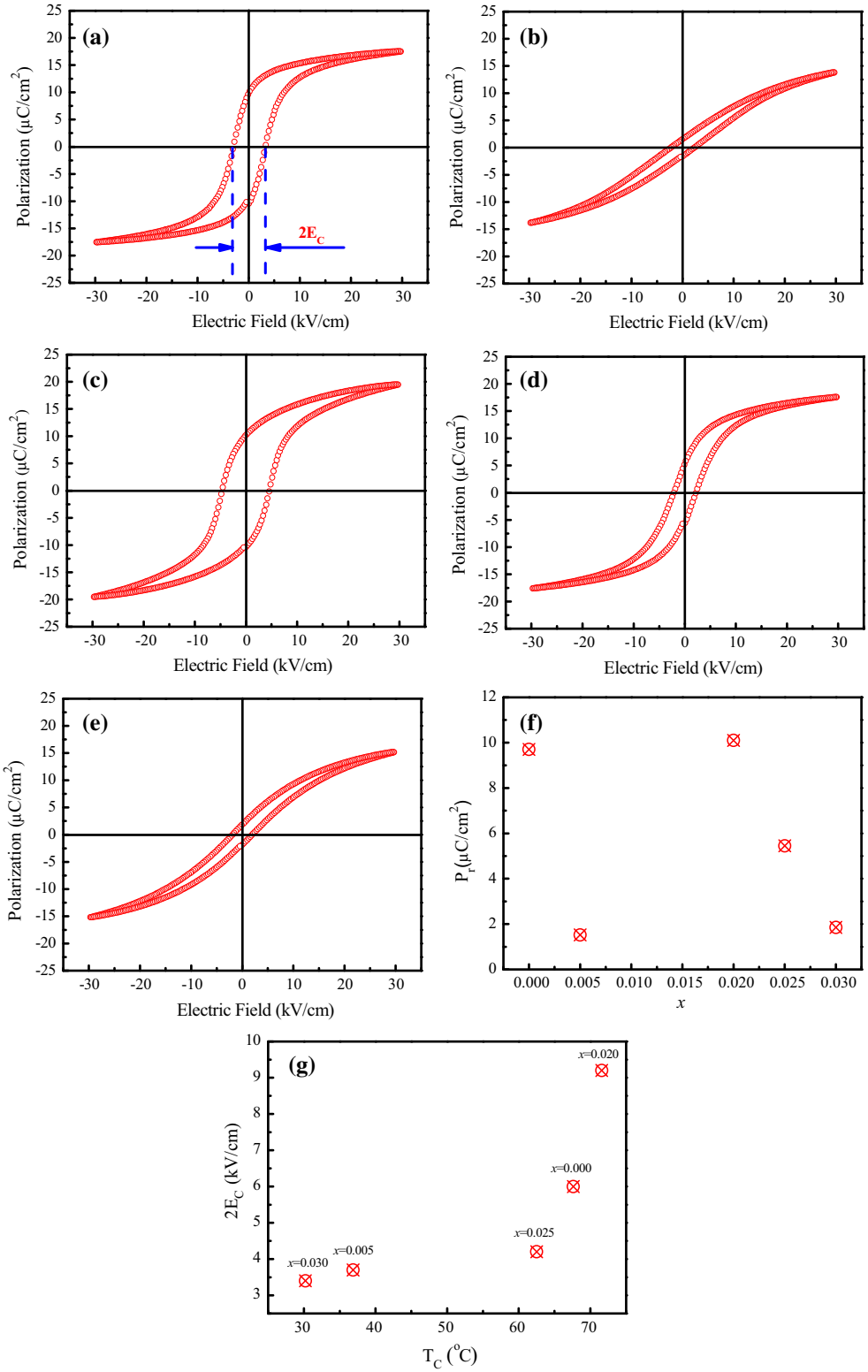

Fig. 6 P–E loops of the $Ba_{0.9}Ca_{0.1}Ti_{0.9}Zr_{0.1}O_3$–$xBi^{3+}$ ceramics with different x: (a) $x = 0.000$; (b) $x = 0.005$; (c) $x = 0.020$; (d) $x = 0.025$; (e) $x = 0.030$

high voltage, which is agreed with the conclusion of our early studies [10, 11]. Sample with $x = 0.020$ shows a maximum value of $P_r = 10.10$ μC/cm^2 and the minimum value of $P_r = 1.52$ μC/cm^2 exists in sample with $x = 0.005$, and the relationship between x and P_r is shown in (f). To characterize the breadth of P–E loops, the

relationship between T_C and $2E_C$ is illustrated in (g): A novel conclusion can be obtained that the $2E_C$ increases with increasing T_C. It is known to all that in normal ferroelectrics, the ferroelectric properties such as P–E loops can only be detected under T_C (ferroelectric phase) while in relaxor ferroelectrics it can be observed in all the T_C range, even at temperature over T_C, for the existence of ferroelectric domains in all the T_C range. In T_C peak, the amounts of ferroelectric domains decreases and the ferroelectric properties weakens with increasing temperature, and it can be deduced that the P–E loops will be narrower and finally be a single line with the T_C moving to lower temperature [10–15].

The variations of the d_{33} with different x except for 0.010 and 0.015 for the $Ba_{0.9}Ca_{0.1}Ti_{0.9}Zr_{0.1}O_3$–$xBi^{3+}$ ceramics are shown in Fig. 7. Piezoelectric properties can not be detected as well in samples with $x = 0.010$ and $x = 0.015$ for the same reason in Fig. 6. Sample for $x = 0.025$ exhibits the maximum value of d_{33} for the coexistence of orthorhombic and tetragonal phase while the d_{33} in $x = 0.000$ and $x = 0.020$ samples is much lower, and the samples for $x = 0.005$ and $x = 0.030$ show the medium value of d_{33}. That is because the piezoelectrics exhibit optimistic piezoelectric properties near the morphotropic phase boundary (MPB) [3, 13–19]. $Ba_{0.9}Ca_{0.1}Ti_{0.9}Zr_{0.1}O_3$–$0.025Bi^{3+}$ possesses the coexistence of orthorhombic and tetragonal phase thus show higher d_{33}, and the inferior piezoelectric properties of sample for $x = 0.000$ and $x = 0.020$ results from the single orthorhombic phase at room temperature. The $x = 0.005$ and $x = 0.030$ samples also possess higher d_{33} for the coexistence tetragonal and cubic phase. As discussed above, these two samples are also excellent relaxor ferroelectrics and in this case, piezoelectric materials with dielectric relaxor behavior were obtained.

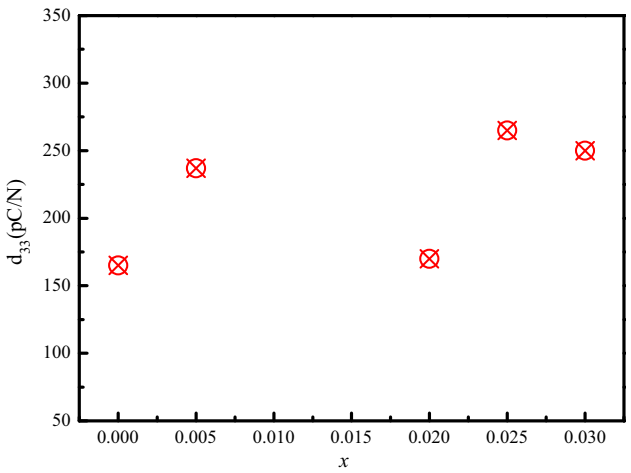

Fig. 7 Piezoelectric coefficient d_{33} of the $Ba_{0.9}Ca_{0.1}Ti_{0.9}Zr_{0.1}O_3$–$xBi^{3+}$ ceramics with different x: (a) $x = 0.000$; (b) $x = 0.005$; (c) $x = 0.020$; (d) $x = 0.025$; (e) $x = 0.030$

4 Conclusions

Lead-free $Ba_{0.9}Ca_{0.1}Ti_{0.9}Zr_{0.1}O_3$–$xBi^{3+}$ ceramics have been prepared by hydrothermal method and the effects of Bi^{3+} on the phase transition, microstructure, dielectric relaxation behavior, ferroelectric and piezoelectric properties of these ceramics were studied. Samples with $x = 0.000$ and $x = 0.020$ possess orthorhombic phase and show poor piezoelectric properties at room temperature. The $Ba_{0.9}Ca_{0.1}Ti_{0.9}Zr_{0.1}O_3$–$0.010Bi^{3+}$ and $Ba_{0.9}Ca_{0.1}Ti_{0.9}Zr_{0.1}O_3$–$0.015Bi^{3+}$ ceramics exhibit giant dielectric behavior and have advantages in lower dielectric loss over CCTO, but are not ferroelectrics nor piezoelectrics. Sample for $x = 0.025$ show coexistence of orthorhombic and tetragonal phase and exhibits the maximum value of d_{33}. Samples with $x = 0.005$ and 0.030 exhibit excellent dielectric relaxation behavior and the relaxation parameters were obtained. These two samples also shows better d_{33} and in this case, the piezoelectric materials with dielectric relaxation behavior were obtained.

Acknowledgments This research was supported by the National Natural Science Foundation of China (51372144 and 51102159), the New Century Excellent Talents Program of Chinese Education Ministry (NCET-11-1042), the International Science and Technology Cooperation Project Funding of Shaanxi Province (2012KW-06), and Graduate Innovation Fund of Shaanxi University of Science and Technology.

References

1. J. Lee, S. Lee, V.A. Hackley, U. Paik, Influence of [Ba+Ca]/[Ti+Zr] ratio on the interfacial property of (Ba,Ca)(Ti,Zr)O3 (BCTZ) powders in an aqueous medium. J. Am. Ceram. Soc. **86**(6), 1034–1036 (2003)
2. L.F. Zhu, B.P. Zhang, X.K. Zhao, L. Zhao, P.F. Zhou, J.F. Li, Enhanced piezoelectric properties of $(Ba_{1-x}Ca_x)(Ti_{0.92}Sn_{0.08})O_3$ lead-free ceramics. J. Am. Ceram. Soc. **96**(1), 241–245 (2013)
3. J.G. Wu, D.Q. Xiao, W.J. Wu, J.G. Zhu, J. Wang, Effect of dwell time during sintering on piezoelectric properties of $(Ba_{0.85}Ca_{0.15})(Ti_{0.90}Zr_{0.10})O_3$ lead-free ceramics. J. Alloys. Compd. **509**, 359–361 (2011)
4. J.G. Wu, D.Q. Xiao, W.J. Wu, Q. Chen, J.G. Zhu, Z.C. Yang, J. Wang, Composition and poling condition-induced electrical behavior of $(Ba_{0.85}Ca_{0.15})(Ti_{1-x}Zr_x)O_3$ lead-free piezoelectric ceramics. J. Eur. Ceram. Soc. **32**, 891–898 (2012)
5. S.O. Leontsev, R.E. Eitel, Progress in engineering high strain lead free piezoelectric ceramics. Sci. Technol. Adv. Mater. **11**, 044302 (2010)
6. Z. Aurang, J.M. Steven, Stability of high-temperature dielectric properties for $(1-x)Ba_{0.8}Ca_{0.2}TiO_3$–$xBi(Mg_{0.5}Ti_{0.5})O_3$ ceramics. J. Am. Ceram. Soc. **96**(9), 2887–2892 (2013)
7. J.G. Wu, W.J. Wu, D.Q. Xiao, J. Wang, Z.C. Yang, Z.H. Peng, Q. Chen, J.G. Zhu, (Ba, Ca)(Ti, Zr)O_3–$BiFeO_3$ lead-free piezoelectric ceramics. Curr. Appl. Phys. **12**, 534–538 (2012)

8. Z. Aurang, J.M. Steven, Dielectric and piezoelectric properties of $(1-x)K_{0.5}Bi_{0.5}TiO_3$–$xBa(Ti_{0.8}Zr_{0.2})O_3$ ceramics. J. Am. Ceram. Soc. **96**(10), 3089–3093 (2013)
9. T. Takenaka, H. Nagata, Current status and prospects of lead-free piezoelectric ceramics. J. Eur. Ceram. Soc. **25**, 2693–2700 (2005)
10. Z.X. Sun, Y.P. Pu, Z.J. Dong, Y. Hu, X.Y. Liu, P.K. Wang, M. Ge, Dielectric and piezoelectric properties and PTC behavior of $Ba_{0.9}Ca_{0.1}Ti_{0.9}Zr_{0.1}O_3$–$x$La ceramics prepared by hydrothermal method. Mater. Lett. **118**, 1–4 (2014)
11. S. Su, R.Z. Zuo, S.B. Lu, Z.K. Xu, X.H. Wang, L.T. Li, Poling dependence and stability of piezoelectric properties of $Ba(Zr_{0.2}Ti_{0.8})O_3$–$(Ba_{0.7}Ca_{0.3})TiO_3$ ceramics with huge piezoelectric coefficients. Curr. Appl. Phys. **11**(3), S120–S123 (2011)
12. D.M. Finlay, C.S. Derek, R.W. Anthony, An alternative explanation for the origin of the resistivity anomaly in La-doped $BaTiO_3$. J. Am. Ceram. Soc. **84**(2), 474–476 (2001)
13. R.Z. Zuo, X.S. Fang, C. Ye, Phase structures and electrical properties of new lead free $(Na_{0.5}K_{0.5})NbO_3$–$(Bi_{0.5}Na_{0.5})TiO_3$ ceramics. Appl. Phys. Lett. **90**, 092904 (2007)
14. J. Wu, D. Xiao, W. Wu, Q. Chen, J. Zhu, Z. Yang, J. Wang, Role of room-temperature phase transition in the electrical properties of (Ba, Ca)(Ti, Zr)O_3 ceramics. Scr. Mater. **65**, 771–774 (2011)
15. Y.C. Lee, Y.Y. Yeh, P.R. Tsai, Effect of microwave sintering on the microstructure and electric properties of (Zn, Mg)TiO_3-based multilayer ceramic capacitors. J. Eur. Ceram. Soc. **32**, 1725–1732 (2012)
16. C.Y. Tsay, K.S. Liu, I.N. Lin, Microwave sintering of $(Bi_{0.75}Ca_{1.2}Y_{1.05})(V_{0.6}Fe_{4.4})O_{12}$ microwave magnetic materials. J. Eur. Ceram. Soc. **24**, 1057–1061 (2004)
17. T. Chen, T. Zhang, G. Wang, J. Zhou, J. Zhang, Y. Liu, Effect of CuO on the microstructure and electrical properties of $Ba_{0.85}Ca_{0.15}Ti_{0.90}Zr_{0.10}O_3$ piezoceramics. J. Mater. Sci. **47**, 4612–4619 (2008)
18. P. Wang, Y.X. Li, Y.Q. Lu, Enhanced piezoelectric properties of $(Ba_{0.85}Ca_{0.15})(Ti_{0.9}Zr_{0.1})O_3$ lead-free ceramics by optimizing calcination and sintering temperature. J. Eur. Ceram. Soc. **31**, 2005–2012 (2011)
19. J. Tao, Z.G. Yi, Y. Liu, M.X. Zhang, J.W. Zhai, Dielectric tunability, dielectric relaxation, and impedance spectroscopic studies on $(Ba_{0.85}Ca_{0.15})(Ti_{0.9}Zr_{0.1})O_3$ lead-free ceramics. J. Am. Ceram. Soc. **96**(6), 1847–1851 (2013)